Heliyon 6 (2020) e03228

Contents lists available at ScienceDirect

Heliyon

journal homepage: www.cell.com/heliyon

Research article

Characterization of lignin enforced tannin/furanic foams

Toni Varila [b,*], Henrik Romar [a], Tero Luukkonen [c], Tuomo Hilli [d], Ulla Lassi [a,b,**]

[a] University of Oulu, Research Unit of Sustainable Chemistry, P.O. Box 8000, FI-90014, University of Oulu, Finland
[b] University of Jyvaskyla, Kokkola University Consortium Chydenius, Applied Chemistry, P.O. Box 567, FI-67101, Kokkola, Finland
[c] University of Oulu, Fibre and Particle Engineering Research Unit, P.O. Box 8000, FI-90014, University of Oulu, Finland
[d] Fifth Innovation Oy, P.O. Väinölänkatu 2685, FI-33500, Tampere, Finland

ARTICLE INFO

Keywords:
Materials chemistry
Organic chemistry
Lignin
Tannin
Mechanical strength
Physical activation
Pore development

ABSTRACT

Worldwide, tons of lignin is produced annually in pulping plants and it is mainly considered as a waste material. Usually lignin is burned to produce energy for the pulping reactors. The production of value-added materials from renewable materials like lignin, has proved to be challenging. In this study, the effects of addition of three different types of lignin in the production of tannin/furanic foams is investigated. The foams were matured, first at 373 K and finally carbonized at 1073 K and the properties of them including mechanical strength, specific surface area and pore development are investigated before and after thermal treatment. According to the results, higher mechanical strength is obtained if samples are carbonized at 1073K compared to matured ones at 373K. Up to 10 times stronger materials are achieved this way, which makes them promising as insulating or constructive materials. With physical activation, it is possible to obtain specific surface areas and pore volumes close to 1200 m^2/g and 0,55 cm^3/g respectively. Mainly micropores are developed during the steam activation which makes these foams more suitable and selective to be used as catalyst support materials in the catalytic conversion of small molecules or in adsorption or gas storage application.

1. Introduction

It is a fact, that fossil fuels are depleting fast and efforts are already been taken to overcome this issue [1]. Development of new greener ways to produce biofuels using biomass based heterogeneous catalyst in reactions, has grown tremendously in the 21st century. In the past, various biomass supported catalyst has been produced and tested in some applications. For instant, nutshells [2], lignin [3] and sucralose [4] based carbon catalysts have been successfully tested previously with high conversion rates (55–65 %) in bioethanol production.

Wood and pulping/paper industries produces in large scale a lot of by-products, such as lignin and tannins, which are considered as low value products especially lignin [5, 6]. Lignin is highly branched polymer that consist of three main building block, presented in Figure 1, and are mostly linked together via b-aryl ether linkages (b-O-4).

In wood structure, lignin can be found in the middle lamella and in the cell walls of the wood [7]. After cellulose, lignin is the second abundant material in wood chemical structure and depending on the wood species, spruce, birch, pine or other species, the lignin content varies from 15 to 25 % of total mass of the wood [7, 8]. Until now, the main usage of lignin, for example in paper industry, is burning it to produce energy for the pulping boilers [9]. High value products like lignosulfonates, derivated from sulphite pulping, and their usage in concrete and cement industry as plasticizers is so far the most useful application for lignin even if the production is decreasing due to the decrease in number of sulphite plants[10]. Other application such as, production of activated carbon, phenols and carbon fibers from lignin has also gained a lot of interest during the last few years. Recently, Merle *et al.* [6] studied lignin-tannin based foams and their physical properties such mechanical strength and thermal conductivity.

Chemistry of lignin is complicated and the scientist propose one after another a more accurate ways to demonstrate the actual structure of lignin and its reactivity to find better end use applications for it. The most common linkages in spruce lignin structure are α and β-O-4 ether linkages, aliphatic and phenolic OH-groups, which are linked to the phenylpropane skeleton as presented in Figure 2 [11]. The reactivity of these linkages or groups varies greatly, which must take into account to understand the chemistry behind the synthesis of tannin-lignin based foams. According to the literature, most reactive sites in lignin are the phenolic α-O-4 linkages and far less reactive are the phenolic β-O-4

* Corresponding author.
** Corresponding author.
E-mail addresses: toni.varila@chydenius.fi (T. Varila), ulla.lassi@oulu.fi (U. Lassi).

https://doi.org/10.1016/j.heliyon.2020.e03228
Received 20 August 2019; Received in revised form 21 October 2019; Accepted 10 January 2020

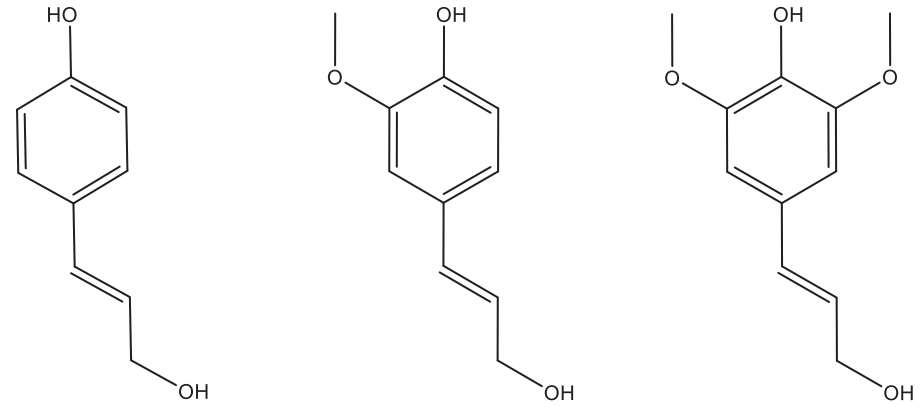

Figure 1. Basic building blocks for lignin polymer.

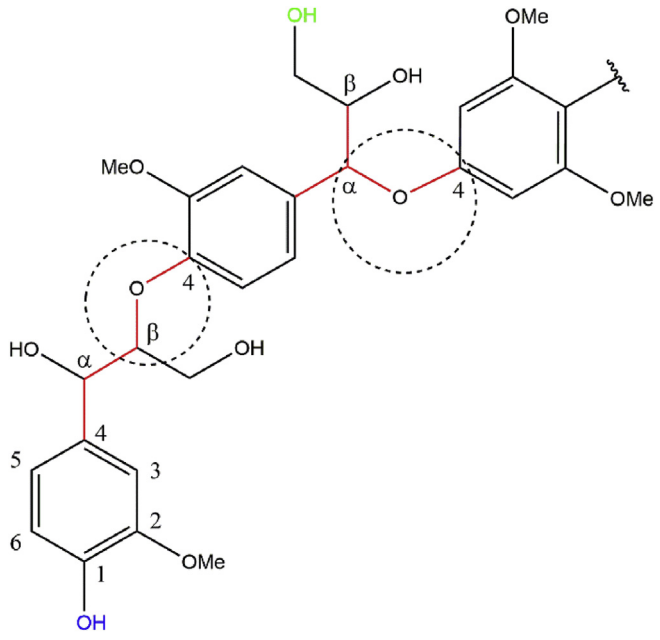

Figure 2. The most reactive bonds types in lignin structure are α-O-4 (right circle), β-O-4 (left circle), aliphatic (green) and phenolic (blue) OH-groups.

linkages in alkaline solutions [12]. In acidic solution, condensation reaction or cleavage of α-O-4 and β-O-4 linkages into monomeric lignin fragments can occur, which can then further react with other molecules, such as aldehydes, as suggested by Li *et al.* [13] Based on this, furfuryl alcohol, that is used in the foaming process, might react with the phenolic lignin fragments that are formed in acidic condition. The suggested reaction mechanism for furfural alcohol and lignin fragments under acidic condition is presented in Figure 3.

Tannins are defined as water soluble phenolic compounds that exists in fruits, woods, seeds and in many vegetable oils. Tannins, can by divided in three groups by their native structure: hydrolysable tannins, condensed tannins and phlorotannins. Hydrolysable tannins consist of several gallic acid or ellagic acid units linked to the central D-glucose core via ester bonds, as presented in Figure 4a. They have relatively high phenol content due to gallic or ellagic acid units [14, 15, 16, 17]. Recently, Varila *et al.* [18] studied the behavior of hydrolysable tannin in foaming process using different catalyst and the properties of these foams. Structurally, phlorotannins are the simplest of all the tannins. They consist of one or more phloroglucinol units (Figure 4b), found mainly in marine organisms [19], that are attached to each other via C–C or C–O–C bonds.

The structure of condensed tannins is well known. Basic structure of condensed tannin is cathecin or epicatechin molecule. They have 15 carbon atoms arranged in three rings, as can been seen from Figure 4c [14, 20]. Use of condensed tannins in foaming application and properties, such as fire resistance, adsorption of metals, permeability, conductivity, mechanical strength, and formulations of them has been widely studied in the past by many authors [21, 22, 23, 24, 25, 26].

In the synthesis of tannin-based foams, the key ingredients are cross-linking agents, which can be for example aldehydes or alcohols such as formaldehyde, glutaraldehyde or furfuryl alcohol. These agents are responsible for the porous like structure, which is forming during the polymerization reaction between the individual condensed or hydrolysable tannin molecules. Glutaraldehyde or furfural alcohol are preferred in the polymerization reaction more than formaldehyde due to the toxicity of and environmental impact of it. For furfuryl alcohol, two possible reactions can occur during the polymerization. First is the heat-generating auto-polymerization reaction between furfural molecules and later on reaction with free aromatic OH-groups of condensed or hydrolysable tannin molecule under acid conditions [23, 27]. The detailed reaction mechanism between furfural alcohol and tannic acid is described by Varila *et al.* [18] The actually foaming or bubble formation inside the foam is created by adding a blowing agent, which is usually low-boiling aliphatic hydrocarbons such as pentane, hexane or organic solvents such as diethyl ether. During the exothermic polymerization under acid condition, heat is generated which evaporates the blowing agent and raises the foam [24, 28].

One challenge with the carbon foams produced from pure tannic compounds is the lack of mechanical strength. In fact, the tannin-furanic foams as such are rather brittle as previously reported [22, 26]. The thermal treatment at high temperatures (1073 K and above), will to some extent increase the mechanical stability of the foams [18]. Carbon foams produced by polymerization reaction of phenols and formaldehyde have been proved to have high mechanical stability as described by [30]. The polyphenolic molecule lignin can undergo polymerization reactions similar to the ones described for other tannin molecelus [18].

In this curiosity-driven work, a new type of lignin enforced tannin-furanic foams are presented. The foams are produced using different types of Kraft lignin and hydro thermally modified Kraft lignin in combination with hydrolysable tannins inside the foam. The aim of this article is to demonstrate that these lignin-tannin-furanic based foams have a mechanical strength better than the standard tannin-based foams, and that these enforced carbon foams can be thermally stabilized for high mechanical strength. Some of the lignin-tannin foams are thermally carbonized and converted to activated carbon foams by physical

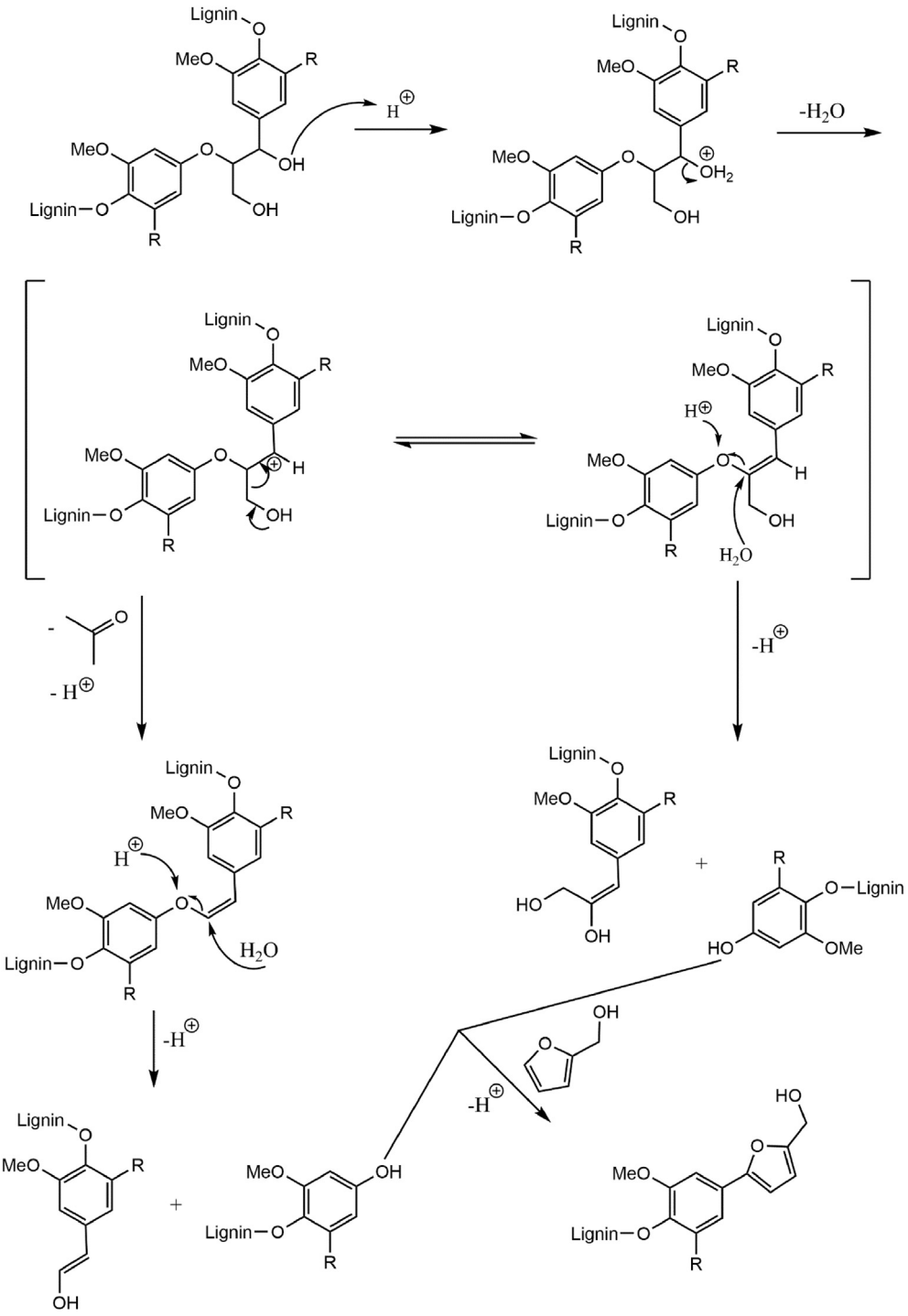

Figure 3. Suggested reaction mechanism for phenolic part of lignin and furfuryl alcohol at acidic conditions.

activation in order to investigate the effect of different lignin types and their amount on the specific surface area, pore volume and pore size distribution of the foams.

2. Material and methods

The commercial tannin acid (95 %), furfuryl alcohol (98%), surfactant (Tween 85) used in the experiments were ordered from Acros Organic. Catalyst, para- toluene sulfonic acid monohydrate (PTSA), and blowing agent (n-pentane) were ordered from Merck Company. Three types of lignin LBS (Lignoboost Kraft lignin) extractions from softwood (pine and spruce), LBD (Lignoboost kraft) extractions from pine wood, and LBHT (Lignoboost hydrothermal lignin) were obtained from pulping mills.

2.1. Preparation of the lignin-tannin-furanic foams (LTFF)

Lignins, LBS (S), LBD (D), LBHT (HT), were oven dried at 373 K over night before use. In total, 9 different tannin-furanic foams (TFF) were prepared having a different lignin/tannin ratios (10 w%, 25 w% and 50 w %). Ratios were calculated by mixing different amounts of lignin with a constant mass of tannin acid. Compositions of each foams are presented

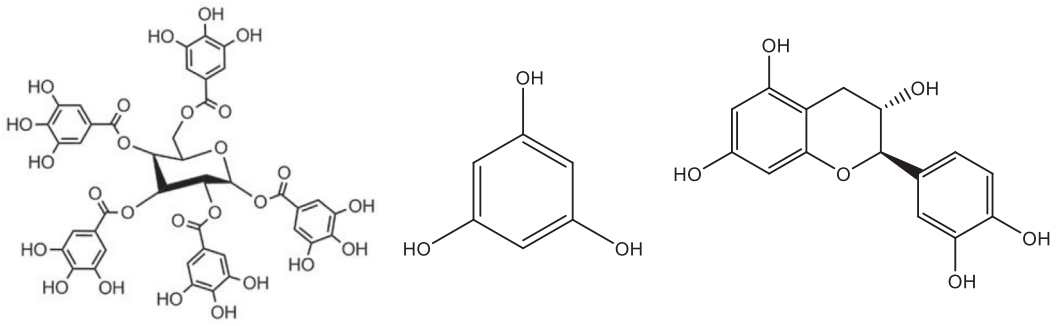

Figure 4. Different tannin types divided, based on their structure, into three categories [14].

in Table 1. Samples were named after the type of lignin (S, D or HT) used in the preparation of TFFs and after the lignin/tannin ratios inside the individual foam 1 = 10 w%, 2 = 25 w% and 3 = 50 w%. For example, TFFD3 correspond to a tannin-furanic foam prepared with LBD-lignin with a lignin/tannin ratio of 50 w%.

In 1-L beaker, water, furfuryl alcohol and Tween 85 were added and mixed thoroughly until homogenous solution was obtained. To this mixture, tannin acid and lignin, depending on the sample that was prepared, were added and the mixture was strongly agitated with mechanical stirrer at 2000 rpm for 5 min. Blowing agent (n-pentane) was poured in to the mixture and the stirring was continued until the mixture stabilized, this stage did not take longer than few seconds. Finally, the catalyst was added and the mixture was mixed well for 5–10 s. The polymerization reaction occurred within 30 s and the reaction was highly exothermic. After the rising has stopped, foams were matured in an oven under natural convention at 373 K for 24 h.

2.2. Thermal stabilization and steam activation of the foams formed

After the maturing, each LTFF were cut into rectangular shapes with palette knife and placed in a stainless-steel fixed-bed reactor for a combination of carbonization and physical (steam) activation or for carbonization only. The reactor was placed in a tubular oven (Nabertherm RT 50) and flushed with inert gas (N2) in order to avoid oxidation of the samples. In total, 18 LTFF samples were produced, 9 samples were carbonized at 1073 K followed by 2 h steam activation at the target temperature using 0.50 ml/min flowrate of water. The other 9 samples were carbonized for 2 h at 1073 K without activation. Afterwards samples were further analyzed regarding the specific surface area, pore volumes and pore size distributions. Due to the fragility and the shrinkage of LTFFs during the carbonization process, the precise dimension cut (3 cm × 3 cm x 3 cm) of matured and carbonized LTFFs was made after the carbonization in order to make comparison in mechanical strength between them.

Table 1. Formulation of LTFFs. PTSA = para-toluene sulfonic acid monohydrate.

Sample	Tannin acid (g)	Furfuryl alcohol (g)	Tween 85 (g)	LBS (g)	LBD (g)	LBHT (g)	Water (g)	n-pentane (g)	PTSA (65%)(g)
TFFS 1	27	14	2	3	-	-	9	4.5	8
TFFS 2	22.5	14	2	7.5	-	-	9	4.5	8
TFFS 3	15	14	2	15	-	-	9	4.5	8
TFFD 1	27	14	2	-	3	-	9	4.5	8
TFFD 2	22.5	14	2	-	7.5	-	9	4.5	8
TFFD 3	15	14	2		15	-	9	4.5	8
TFFHT 1	27	14	2	-	-	3	9	4.5	8
TFFHT 2	22.5	14	2	-	-	7,5	9	4.5	8
TFFHT 3	15	14	2	-	-	15	9	4.5	8

Table 2. Comparison of compression stability between matured and carbonized LTFFs.

Sample	Matured foams			Carbonized foams		
	Compressive strength (MPa)	Elastic modulus (MPa)	Density (g/cm^3)	Compressive strength (MPa)	Elastic modulus (MPa)	Density (g/cm3)
TFFS 1	0.049	0.0035	0.083	0.35	0.080	0.099
TFFS 2	0.045	0.0019	0,053	0.22	0.0070	0.055
TFFS 3	0.037	-[a]	0.133	0.18	0.016	0.127
TFFD 1	0.037	0.0043	0.06	0.21	0.0137	0.057
TFFD 2	0.046	0.0067	0.051	0.23	0.011	0.043
TFFD 3	0.095	0.070	0.170	0.20	0.15	0.171
TFFHT 1	0.036	0.0036	0.046	0.15	0.0083	0.046
TFFHT 2	≈0[b]	≈0[b]	0.11	0.27	0.018	0.087
TFFHT 3	0.046	-[a]	0.212	0.46	0.29	0.195

[a] = no clear linear region in the stress-strain curve, b = sample was too fragile to be measured.

2.3. Determination of compression stability of the LTTFs

Compressive strengths of foams were determined using a Zwick/Roell Z010 testing machine (with a load cell of 10 kN). The loading speed was 0.1 mm/s and the measurement ended when the force decreased by 50 % from maximum or deformation reached 30 %. Compressive strength was calculated with Eq. (1).

$$\text{Compressive strengths (MPa)} = F/A \quad (1)$$

where F (N) is the maximum force at the linear region of the compression curve and A (mm^2) is the surface area.

2.4. Specific surface areas and pore size distributions

After the careful sample preparation, Micromeritics ASAP 2020 instrument was used to determine the specific surface area, pore volume and pore size distributions from the adsorption isotherms using nitrogen as adsorbate. Prior to the measurement, degassing process for each sample (200 mg) was carried out at low pressure (2 μm Hg) and at temperature of 413 K for 2 h. Degassing of the sample is needed in order clean the surface and pores from adsorbed gas trapped inside the porous structure of the sample. Each sample, after degassing stage, was immersed to liquid nitrogen (77,15 K) at low pressure and nitrogen gas was added in small doses in order to fill the pores inside the samples. After the measurement, specific surface area can be calculated from the adsorption isotherms according to the BET method [31] while the pore size distributions were calculated using the DFT (Density Functional Theory) algorithm [32] assuming slit-formed pores [33]. Total pore volumes were calculated at a P/P0 ratio of 0.985 and in case of DFT as the total volume of pores measured at maximum pore width. The t-plot calculation for the activated carbon were done using Harkins and Jura equations [34]. Pore widths down to 1.5 nm can be accurately measured with the instrument settings.

2.5. Calculation of relative density of LTTFs

Densities of each foam were measured right after the maturation and after the carbonization of the lignin based tannin furanic foams. Measuring the total volume and weight of each sample, densities are obtained from Eq. (2), which can be defined as,

$$\rho = m/V, \quad (2)$$

where m is the mass of the sample and V is the total volume obtained by measuring the dimensions, length, height and width of each rectangular shape tannin furanic foam.

3. Results and discussion

3.1. Compression stability and densities of matured and carbonized LTTFs

According to the results, there is a clear difference in compressive strength between matured and carbonized LTTFs, which is in agreement with earlier published results [18, 25]. Lignin types, S, HT and D used in the formulation of foams, had significant effect on the mechanical strengths, densities and elastic modulus of the foams. As can be seen from Table 2, increasing the amount of S-lignin, from 10 w% to 50 w%, mechanical strength and elastic modulus decreased but density increased. This finding can be seen in both matured -and carbonized foam samples. Increasing D-lignin amount, from 10 w% to 50 w% in matured samples, all physical properties, mechanical strength, density and elastic modulus, are increasing. Carbonized D-lignin samples had similar mechanical strength despite the D-lignin amount but an increase in density and elastic modulus was observed. With HT-lignin, a slight increase in mechanical strength, density and elastic modulus of matured samples was noticed. This observation can be seen even clearer from carbonized

Table 3. Comparison of specific surface area (SSA), pore volume (PV) and pore size distribution between carbonized and steam activated LTTFs.

Calculation method	Unit	Samples															
		Carbonized							Activated								
		TFFS1	TFFS2	TFFS3	TFFHT1	TFFHT2	TFFHT3	TFFD1	TFFD2	TFFD3	TFFS1	TFFS2	TFFS3	TFFHT1	TFFHT2	TFFHT3	TFFD1	TFFD2	TFFD3
BET																			
SSA	m^2g^{-1}	407	0.001	0.14	252	100	0.21	100	12.6	*	803	823	737	671	749	537	737	1179	940
Pore volume	cm^3g^{-1}	0.176	*	*	0.1	0.037	*	0.043	0.005	*	0.338	0.345	0.323	0,306	0.351	0.322	0.313	0.550	0.439
t-plot																			
Micropore volume	cm^3g^{-1}	0.143	*	*	0.09	0.035	*	0.031	*	*	0.289	0.293	0.275	0.232	0.252	0.157	0.264	0.375	0.316
Micropore area	m^2g^{-1}	355	*	*	240	98	*	87	*	*	715	726	681	575	625	388	653	934	784
External surface area	m^2g^{-1}	52	*	*	12	2	*	13	*	*	88	97	86	96	124	150	84	244	156
DFT																			
Pore volume	cm^3g^{-1}	0.145	*	*	0.091	0.032	*	0.045	0.0038	*	0.279	0.287	0.267	0.252	0.290	0.269	0.258	0.449	0.356
Micropores	%	94.5	*	*	91.2	97	*	66.6	92.1	*	97.8	97.6	97.7	88.5	85.5	61.3	96.9	87.1	88.2
Mesopores	%	5.5	*	*	2.2	3	*	20.0	0	*	2.2	2.4	2.3	11.5	14.5	38.7	2.7	12.9	11.5
Macropores	%	0	*	*	6.6	0	*	13.3	7.9	*	0	0	0	0	0	0	0.3	0	0.3

* = Instrument was unable to measure the value. Value too small.

HT-samples. At 50 w% of HT-lignin, mechanical strength, 0.46 MPa, density, 0.195 g/cm^3 and elastic modulus, 0.29 MPa, were obtained. These values indicates that when using HT-lignin in foam formulation the best physical properties, mechanical strength, density and elastic modulus are achieved.

Earlier research on tannin foams has indicated that higher compressive strength can be obtained if bulk density is increased [27] cell size is decreased [35], or certain aminated additives or surfactants are used [36]. The compressive strengths of tannin foams in earlier studies have ranged from 0.03 to 3.97 MPa [22] and thus the results of the present study is in good agreement with those. However, the elastic moduli are clearly lower than obtained for instance by Santiago-Medina et al [36]. Thus, resistance against non-permanent deformation is low, that is, the studied foams exhibit brittle behavior.

As mentioned above, many authors have clearly shown that the mechanical strength of tannin furanic foams are highly dependent on their bulk densities. The results obtained, Table 2, are in some extent in line with the earlier studies [25, 35, 37] Interestingly, if comparing the compressive strength of matured and carbonized samples. There is no significant difference in bulk densities of matured and carbonized samples but despite this up to 10 times, stronger material can be achieved with carbonization process. In addition, elastic modulus in all sample increases up to three times from their initial state. One possible reason for this can be the shrinkage, (20–30 v%) of tannin furanic foams during the carbonization. More rigid and mechanical stable structure is obtained in this way.

3.2. Physical activation and pore size distribution of the LTFFs

As reported in Table 3 poor specific surface area and pore development is obtained if the LTFFs are carbonized at 1073 K without activation. Increasing the lignin/tannin ratio from 10 w% to 50 w%, for carbonized samples, the specific surface areas and pore volumes decreases significantly. This observation can be made for all lignin types used in the experiments. One of the possible reasons for this might be that the lignin is sheltering the tannin-furanic structures and therefor preventing the development of porosity during the carbonization or it is harder to develop pores inside the lignin structure.

Based on the results, the best specific surface area and pore volumes for activated samples are obtained using 25 w% lignin/tannin ratio in all cases. Highest pore volume and specific surface area, was obtained using 25 w% D-lignin ratio, 0.55 cm^3/g and 1179 m^2/g respectively, and the lowest with HT-lignin, 0.35 cm^3/g and 749 m^2/g, in same ratio. It seem that HT-lignin has the highest impact on the pore size distribution. Microporosity decreased from 88.5 % to 61.3% when increasing the lignin amount from 10 w% to 50 w%. On the other hand, mesoporosity increased with the increasing HT-lignin amount from 11.5 % to 38.7 %. Also, slight increase in mesoporosity, from 2.7 % to 12.9% was noticed with increasing D-lignin amount from 10 w% to 25 w%. With the S-type lignin, there seem to be no correlation between the porosity and amount of S-lignin used in the formulation. Based on the results, these foams are more suitable and selective to be used as catalyst support materials in the catalytic conversion of small molecules. On the other hand, specific surface areas for activated LTFFs are comparable with commercial activated carbons. Furthermore, they have relatively good pore volumes which plays a key role in some application such as adsorption of metal from wastewaters or in gas storage.

4. Conclusions

In this study, the mechanical strength, density, specific surface area, pore volume and pore size distribution properties of lignin enforced tannin foams was studied. According to the results, carbonized tannin furanic foams with different lignin inside are up to 10 times more stronger than just matured ones. The best specific surface areas and pore volumes are obtained using 25 w% lignin/tannin, with all lignin types. However, pores created during the carbonization were mostly microporous regardless the fact that HT and D-lignin types increased the mesoporosity in some extent.

This study showed that it is possible to use lignin feedstocks to produce a lignin enforced tannin foams with tailored properties and that these foams are more than suitable for numerous applications such as construction, adsorption or gas storing material.

Declarations

Author contribution statement

Toni Varila, Tero Luukkonen: Performed the experiments; Analyzed and interpreted the data; Wrote the paper.

Henrik Romar: Conceived and designed the experiments; Analyzed and interpreted the data; Wrote the paper.

Tuomo Hilli: Contributed reagents, materials, analysis tools or data.

Ulla Lassi: Conceived and designed the experiments.

Funding statement

Toni Varila was supported by the Green bioraff solutions project (EU/Interreg/Botnia-Atlantica, 20201508).

Competing interest statement

The authors declare no conflict of interest.

Additional information

No additional information is available for this paper.

References

[1] R. Chakraborty, S. Chatterjee, P. Mukhopadhyay, S. Barman, Progresses in waste biomass derived catalyst for production of biodiesel and bioethanol: a review, Procedia Environ. Sci. 35 (2016) 546–554.

[2] M. Liu, S. Jia, Y. Gong, C. Song, X. Guo, Effective hydrolysis of cellulose into glucose over sulfonated sugar-derived carbon in an ionic liquid, Ind. Eng. Chem. Res. 52 (24) (2013) 8167–8173.

[3] S. Kang, J. Ye, Y. Zhanga, J. Chang, Preparation of biomass hydrochar derived sulfonated catalysts and their catalytic effects for 5-hydroxymethylfurfural production, RSC Adv. 3 (2013) 7360–7366.

[4] S. Hu, T.J. Smith, W. Lou, M. Zong, Efficient hydrolysis of cellulose over a novel sucralose-derived solid acid with cellulose-binding and catalytic sites, J. Agric. Food Chem. 62 (8) (2014) 1905–1911.

[5] D. Stewart, Lignin as a base material for materials applications: chemistry, application and economics, Ind. Crops Prod. 27 (2008) 202–207.

[6] J. Merle, M. Birot, H. Deleuze, C. Mitterer, H. Carré, F.C. Bouhtoury, New biobased foams from wood byproducts, Mater. Des. 91 (2016) 186–192.

[7] R. Alén, Structure and chemical composition of wood, in: P. Stenius (Ed.), Forest Products Chemistry, Fapet Oy, Helsinki, Finland, 2000, pp. 12–57.

[8] M. Norgren, H. Edlund, Lignin: recent advances and emerging applications, Curr. Opin. Colloid Interface Sci. 19 (2014) 409–416.

[9] E. Brännvall, Overview of pulp and paper processes, in: M. Ek, G. Gellerstedt, G. Henriksson (Eds.), Pulping Chemistry and Technology 2, de Gruyter, 2009, pp. 1–13.

[10] A.L. Macfarlane, M. Mai, J.F. Kadla, 20 - Bio-based chemicals from biorefining: lignin conversion and utilisation, in: K. Waldron (Ed.), Advances in Biorefineries, Woodhead Publishing, 2014.

[11] A. Sakakibara, Y. Sano, in: D. Hon, N. Shirashi (Eds.), Chemistry of Lignin, second ed., Marcel Dekker, New York, 1991, pp. 111–175.

[12] E.I. Evstigneyev, S.M. Shevchenko, Structure, chemical reactivity and solubility of lignin: a fresh look, Wood, Sci. Tech. 53 (2019) 7–47.

[13] Y. Li, L. Shuai, H. Kim, A.H. Motagamwala, J.K. Mobley, F. Yue, Y. Tobimatsu, D. Havkin-Frenkel, F. Chen, R.A. Dixon, J.S. Luterbacher, J.A. Dumesic, J. Ralph, An "ideal lignin" facilitates full biomass utilization, Sci. Adv. 4 (2018), eaau2968.

[14] J. Salminen, 6.6.17, http://naturalchemistry.utu.fi, 2017.

[15] W.J. Kilkowski, G.G. Gross, Color reaction of hydrolyzable tannins with Bradford reagent, Coomassie brilliant blue, Phytochemistry 51 (1999) 363–366.

[16] G.G. Gross, Biosynthesis, biodegradation, and cellular localization of hydrolyzable tannins, in: N.G. Lewis, J.T. Romeo, G.H.N. Towers (Eds.), Phytochemicals in Human Health Protection, Nutrition and Plant Defenses, Plenum Press, New York, 1999, pp. 185–213.

[17] R.V. Barbehenn, C.P. Jones, A.E. Hagerman, M. Karonen, J. Salminen, Ellagitannins have greater oxidative activities than condensed tannins and galloylglucoses at high pH: potential impact on caterpillars, J. Chem. Ecol. 32 (2006) 2253–2267.
[18] T. Varila, H. Romar, T. Luukkonen, U. Lassi, Physical Activation and Characterization of Tannin-Based Foams Enforced with Boric Acid and Zinc Chloride, 2019.
[19] T. Arnold, N. Targett, Marine tannins: the importance of mechanistic framework for predicting ecological roles, J. Chem. Ecol. 28 (2002) 1919–1934.
[20] P. Pietta, Flavonoids as antioxidants, J. Nat. Prod. 63 (2000) 1035–1042.
[21] G. Tondi, C.W. Oo, A. Pizzi, A. Trosa, M.F. Thevenon, Metal adsorption of tannin based rigid foams, Ind. Crops Prod. 29 (2009) 336–340.
[22] G. Tondi, W. Zhao, A. Pizzi, G. Du, V. Fierro, A. Celzard, Tannin-based rigid foams: a survey of chemical and physical properties, Bioresour. Technol. 100 (2009) 5162–5169.
[23] M. Link, C. Kolbitsch, G. Tondi, M. Ebner, S. Wieland, A. Petutschnigg, Formaldehyde-free tannin based foams and their use as lightweight panels, BioResources 6 (2011) 4218–4228.
[24] G. Tondi, A. Pizzi, Tannin-based rigid foams: characterization and modification, Ind. Crops Prod. 29 (2009) 356–363.
[25] A. Celzard, W. Zhao, A. Pizzi, V. Fierro, Mechanical properties of tannin-based rigid foams undergoing compression, Mater. Sci. Eng. A 527 (2010) 4438–4446.
[26] X. Li, A. Pizzi, C. Lacoste, V. Fierro, A. Celzard, Physical properties of tannin/furanic resin foamed with different blowing agents, BioResources 8 (1) (2013) 743–752.
[27] C. Lacoste, M.C. Basso, A. Pizzi, M.-. Laborie, D. Garcia, A. Celzard, Bioresourced pine tannin/furanic foams with glyoxal and glutaraldehyde, Ind. Crops Prod. 45 (2013) 401–405.
[28] C. Lacoste, M.C. Basso, A. Pizzi, A. Celzard, M. Laborie, Natural albumin/tannin cellular foams, Ind. Crops Prod. 73 (2015) 41–48.
[30] L. Shiwen, G. Quangui, S. Jingli, L. Lang, Preparation of phenolic-based carbon foam with controllable pore structure and high compressive strength, Carbon (2010) 2644–2673.
[31] S. Brunauer, P.H. Emmett, E. Teller, Adsorption of gases in multimolecular layers, J. Am. Chem. Soc. 60 (1938) 309–319.
[32] N.A. Seaton, J.P.R.B. Walton, N. Quirke, A new analysis method for the determination of the pore size distribution of porous carbons from nitrogen adsorption measurements, Carbon 27 (1989) 853–861.
[33] C. Lastoskie, K.E. Gubbins, N. Quirke, Pore size heterogeneity and the carbon slit pore: a density functional theory model, Langmuir 9 (10) (1993) 2693.
[34] W.D. Harkins, G. Jura, An adsorption method for the determination of the area of a solid without the assumption of a molecular area, and the area occupied by nitrogen molecules on the surfaces of solids, J. Chem. Phys. 11 (1943) 431.
[35] M. Letellier, C. Delgado-Sanchez, M. Khelifa, V. Fierro, A. Celzard, Mechanical properties of model vitreous carbon foams, Carbon 116 (2017) 562–571.
[36] F.J. Santiago-Medina, C. Delgado-Sánchez, M.C. Basso, A. Pizzi, V. Fierro, A. Celzard, Mechanically blown wall-projected tannin-based foams, Ind. Crops Prod. 113 (2018) 316–323.
[37] C. Lacoste, M.C. Basso, A. Pizzi, M.-. Laborie, A. Celzard, V. Fierro, Pine tannin-based rigid foams: mechanical and thermal properties, Ind. Crops Prod. 43 (2013) 245–250.